12-11-2009

Verification of a Three-Dimensional Statics Model for Continuum Robotics and the Design and Construction of a Small Continuum Robot (SCR)

Ricky (Ricky Lee) Gray

VERIFICATION OF A THREE-DIMENSIONAL STATICS MODEL FOR CONTINUUM ROBOTICS AND THE DESIGN AND CONSTRUCTION OF A SMALL CONTINUUM ROBOT (SCR)

By

Ricky Lee Gray Jr

A Thesis
Submitted to the Faculty of
Mississippi State University
in Partial Fulfillment of the Requirements
for the Degree of Master of Science
in Electrical Engineering
in the Department of Electrical and Computer Engineering

Mississippi State, Mississippi

December 2009

VERIFICATION OF A THREE-DIMENSIONAL STATICS MODEL FOR CONTINUUM ROBOTICS AND THE DESIGN AND CONSTRUCTION OF A SMALL CONTINUUM ROBOT (SCR)

By

Ricky Lee Gray Jr

Approved:

_____	_____
Bryan A. Jones Assistant Professor of Electrical and Computer Engineering (Major Advisor and Director of Thesis)	Robert B. Reese Associate Professor of Electrical and Computer Engineering (Committee Member)
_____	_____
Thomas H. Morris Assistant Professor of Electrical and Computer Engineering (Committee Member)	James E. Fowler Professor of Electrical and Computer Engineering (Graduate Program Director)

_____

Sarah A. Rajala
Dean of the Bagley College of Engineering

Name: Ricky Lee Gray Jr

Date of Degree: December 11, 2009

Institution: Mississippi State University

Major Field: Electrical Engineering

Major Professor: Dr. Bryan A. Jones

Title of Study: VERIFICATION OF A THREE-DIMENSIONAL STATICS MODEL FOR CONTINUUM ROBOTICS AND THE DESIGN AND CONSTRUCTION OF A SMALL CONTINUUM ROBOT (SCR)

Pages in Study: 48

Candidate for Degree of Master of Science

Continuum robots are biologically inspired robots that capture the extraordinary abilities of biological structures such as elephant trunks, octopus tentacles, and mammalian tongues. They are given the term continuum robots due to their ability to bend continuously rather than at specific joints such as with traditional rigid link robots. They are used in applications such as search and rescue operations, colonoscopies, minimal invasive surgeries, and steerable needles. In this thesis, a model that predicts the shape of a continuum robot is presented and verified. A verification system to verify the validity and accuracy of the model is presented which allows easy and accurate measurement of a continuum robot tip position. The model was verified against a flexible rod resulting in an accuracy of 0.61%. Finally, this thesis introduces a novel robot design, consisting of a single rod for the backbone which can be manipulated by applying external forces and torques.

Key words: Biologically inspired robots, Continuum robots, Continuum, Biological, Verification, Model, Static, Statics, Tongues, Trunks, Tentacles, Muscular Hydrostat, Hyperredundant, Robots, Robot

DEDICATION

To Mr. and Mrs. Loden, Mr. and Mrs. Matthews, my friends, and my loving parents

ACKNOWLEDGEMENTS

The author expresses his sincere gratitude to his research associates and his advisor. Krishna, one research associate, thanks is due for your help, support, and passion in assisting me during the many hours of trial and error which led to my success. Thanks is also due to those associates who came to our meetings and were a part of the effort in other ways, Durgapavani Brundavanam, Buddy Jones, Anthony Reisman, and Roberto Orellano. Appreciation is also due to my wonderful friends, without their support and love I would have not made it as easily. Finally, sincere thanks are due to Dr. Bryan Jones, my advisor, for his never ending support and guidance and his family for their love and support.

TABLE OF CONTENTS

LIST OF TABLES

LIST OF FIGURES

CHAPTER 1

INTRODUCTION

Much advancement has been made in traditional rigid link robotic systems and recently in another area of robotics known as continuum robotics [1-5]. Continuum robots are based on biological structures such as tongues, trunks, and tentacles. They are designed to capture the amazing characteristics of these remarkable structures. For example, continuum robot applications in the areas of nuclear [6], medical [7-12], and search and rescue [5] has become increasingly popular because robots with these capabilities can search inside confined spaces much easier than traditional rigid link robots, explore underneath and inside holes, and contort around an object without the shape or size being an obstacle. Just like and elephant can pick up a log with its trunk, a continuum robot can pick up an object by wrapping itself around it.

Unlike traditional rigid link robots, continuum robots are more difficult to model, design, and construct due to their lack of rigidity. Unlike rigid-link robots, their bodies can extend, bend continuously, and in some instances expand. This thesis presents achievements in the field of continuum robotics in areas of modeling, verification, and building.

The second chapter discusses a model for a continuum robot. This model is based on special Cosserat rods which when compared to other models such as the constant curvature model is more accurate in predicting the shape of a rod, because it makes few

geometrical approximations and no mechanical assumptions. The model is split into three sections. The first section is the kinematics section and introduces the linear and angular velocities referenced in the global frame. The second section is the mechanics section. It develops equations for both the forces and the moments. The force balance equation is a summation of all forces acting on the rod. The moment balance equation is a summation of all torques acting on the rod. The third section presents the constitutive equations and initial conditions section. The constitutive equations combine the mechanics and kinematics sections and the initial conditions describe the static physical system being modeled. An ODE solver is then used to solve the set of equations given the derivatives of the position, orientation, shear, and bending. The initial bending is guessed and a torque is calculated based on the tip position. This torque is compared to the known torque calculated from the tip mass and the length of the rod. The guess is changed until the two converge.

The third chapter describes how the model presented in chapter two is verified and details the verification system. In order to verify the model, actual measurements from a physical system must be compared to the results of the model. A verification system was designed to obtain actual measurements. The system consists of four main components: a laser-etched grid, rod clamps, levels, and weights. The laser-etched grid is the main component of the verification. It consists of a 1 mm grid which is used to easily measure the tip position. The rod clamps were laser-etched to have different mounting angles for the purpose of orienting the rod for verification. For example, the rod can accurately be placed horizontal or at other angles such as 45 degrees. The two levels allow alignment of the grid with the vertical axis, while the weights are used to apply a force on

the tip of the rod for different tip loading verification. Using the verification system to obtain accurate results for comparison, the model predicts the shape of the rod with accuracy of .61%. This proves that the model presented is viable for predicting the shape as well as controlling a continuum robot.

The fourth chapter presents a continuum robot design which improves on existing designs. The robot is designed with simplicity and functionality in mind. It is composed of a single rod as a backbone which allows the simplest form of the model to be verified before adding complexity to it such as additional robot components and multisection functionality. Several robot designs are discussed and the reasons for not choosing them. For example, one design called The Elephant's Trunk uses a similar approach. It has multi-cable actuation system which is composed of 8 cables and a spring for each pair of cables. It also requires a dc motor for each cable as well as encoders to keep track of cable lengths. The design presented takes a three cable approach and uses three stepper motors; therefore, it reduces the complexity of the entire robot and because of the components used and the design approach taken, which is discussed in detail in the chapter, there is minimal loss in accuracy. This design is also allows easier verification of our model due to the backbone of the robot being a single rod. Since the model is based on special Cosserat rods, the verification is more straight forward with a correctly design verification system. The model is discussed in the following chapter.

CHAPTER 2

THREE-DIMENSIONAL STATICS MODEL

2.1 Introduction

Tongues [13], trunks [13], and tentacles [1-3] are biological structures [13] termed muscular hydrostats [1-3, 13], have unsurpassed grasping abilities. They can grasp objects of various shapes and sizes [2, 3, 14]. Their compliancy and dexterity are both remarkable characteristics. For instance, an elephant can easily pick up a log with its trunk, yet with grace and ease it can pick up a single piece of grass. These biological structures also have extensive sensory abilities which along with mentioned characteristics allow them to easily and efficiently explore in confined areas, under objects, and reach into areas that would be more difficult for a rigid link robot.

For many years now, researchers have been attempting to capture these amazing characteristics in biologically-inspired robots called continuum robots [1-5]. These robots can be used in a wide variety of applications ranging from remote exploration to nuclear applications. In [6] the design for a robot called the CT Arm is proposed for a nuclear reactor maintenance robot. Continuum robots are becoming widely used in the medical applications such as colonoscopies [8, 9], steerable needles [7, 10], and minimally invasive surgeries [11, 12]. In [8] the author describes a semi-autonomous robot, COLOBOT, for colonoscopies. In [10] the author introduces a new approach for designing steerable needles based on curved concentric tubes.

2.2 Background

There have been several approaches to predicting the shape and controlling continuum robots. The most widely used and accepted model, called the constant-curvature model [1, 8, 10, 15-18], applies a constant arc assumption in order to predict the shape; however, due to the exclusion of gravitational loading in the model [3], the results obtained severely limit the accuracy of the model. This results in significant error in the predicted shape of the robot [3, 10, 19] and when used for controlling a continuum robot [14, 19].

Another model is based on the theory of Cosserat rods [2] from Antman [2, 20]. The popularity of this model has grown because there are few geometrical approximations or mechanical assumptions made about the applicable system [20], leading to a much more accurate model. Accuracy is very important when predicting the shape or controlling of a continuum robot. The special Cosserat rods approach was taken in order to obtain maximum accuracy in tip control and continuum robot shape control. The following summarizes our IROS paper.

2.3 Overview

In this approach, our continuum robot is created using a rod and is characterized by its reference unstretched length. The rod is represented as a curve in three-dimensional space and parameterized by variable s, see **Error! Reference source not found.**. A local coordinate frame located at each point along the rod keeps track of the shape and orientation of the rod. Local vectors, denoted with a superscript l throughout this thesis, $\mathbf{v}^l$ (an-

gular velocities) and $\mathbf{v}^l$ (linear velocities) describe the shear and bending strains associated with each point on the rod. While $v^l_{1\ldots2}$ gives shear strains and v^l_3 gives dilation; $u^l_{1\ldots2}$ gives bending strains and u^l_3 gives torsion.

$$\mathbf{u}^l = \begin{bmatrix} u^l_1 & u^l_2 & u^l_3 \end{bmatrix}^{\mathrm{T}} \tag{1}$$

$$\mathbf{v}^l = \begin{bmatrix} v^l_1 & v^l_2 & v^l_3 \end{bmatrix}^{\mathrm{T}} \tag{2}$$

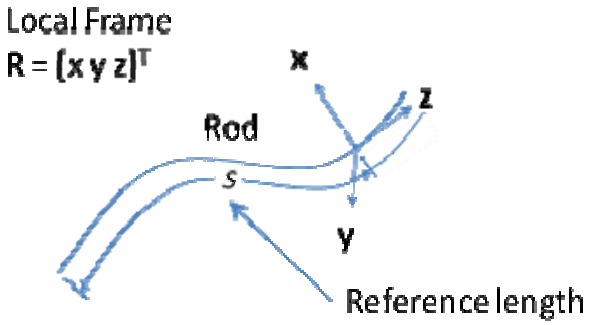

Figure 1. The curve shown represents the rod. It is parameterized by variable *s* and a local coordinate frame is established at each point on the curve. Each point has vectors $\mathbf{u}^l$ and $\mathbf{v}^l$ which describe the shear and bending strains of that particular point. A rotation matrix **R** is used to translate these vectors from a local to global reference frame.

The model for our continuum robot is developed in three sections, kinematics, mechanics, and then constitutive equations along with initial conditions. The Kinematics section provides information about the shape and orientation of the rod due to the bending and shearing caused by forces and moments applied on the rod. The mechanics section provides the force and moment balance equations which in turn define the linear (v) and angular (u) velocities of each point along the rod which are needed for kinematics. The constitutive equations are what combine the mechanics with the kinematics. Fur-

thermore, the initial conditions are used to describe and define the starting shape and orientation of the rod.

2.4 Kinematics

To provide the shape and orientation of a rod, the global angular and linear velocities are needed. As previously discussed, a curve representing a rod is characterized by its reference unstretched length and parameterized by variable s. Representing the location of a point on the rod $\mathbf{r}(s)$ is chosen, see **Error! Reference source not found.**. Also, $\mathbf{R}(s)$ is a rotation matrix that specifies the orientation of the curve with respect to a global coordinate system, thereby a local coordinate frame is attached at each point.

In order obtain the global angular and linear velocities, they are first found in their respective local frames for each discretized point on the curve and then simply multiplied by the rotation matrix. For example, any local vector $\mathbf{a}^l$ can be represented globally by multiplying it by the rotation matrix $\mathbf{R}$ so that $\mathbf{a} = \mathbf{R}\mathbf{a}^l$. Likewise, a global vector $\mathbf{a}$ can be represented locally by multiplying it by the transpose rotation matrix $\mathbf{R}^T$, giving $\mathbf{a}^l = \mathbf{R}^T\mathbf{a}$. Note that the local angular velocities are placed in a skew symmetric matrix. The shear and strain vectors $\mathbf{v}^l$ and $\mathbf{u}^l$ define the change in the position and orientation of the rod so that

$$\dot{\mathbf{r}}(s) = \mathbf{R}(s)\,\mathbf{v}^l(s), \text{ and} \tag{3}$$

$$\dot{\mathbf{R}}(s) = \mathbf{R}(s)\,\hat{\mathbf{u}}^l(s). \tag{4}$$

2.5 Mechanics

2.5.1 Force Balance Equation

A free body diagram allows easily determination of the force balance equation needed for our model; see **Error! Reference source not found.**.

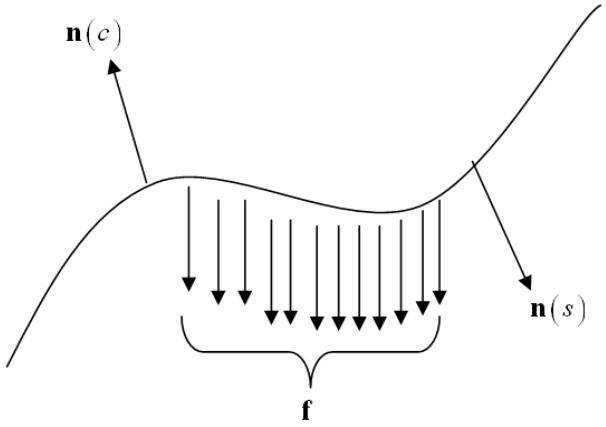

Figure 2 Free body diagram showing contact forces (n(c) and n(s)) and body forces (f)

The force balance equation is composed of all forces acting on the rod from section c to s. Internal forces due to stretching and shearing, called contact forces, are denoted as $\mathbf{n}(c)$ and $\mathbf{n}(s)$. The vector $\mathbf{n}(c)$ represents the force applied on the segment of interest by the rest of the rod from the base to that point; likewise, $\mathbf{n}(s)$ represents the force applied on the segment by the rest of the rod from that point to the end of the rod. All other external forces on applied or acting on the rod are called body forces; for example, a body force created by gravitational loading is one such external force. In Figure 2, these external forces are represented as $\mathbf{f}$ and are summed together in (5) and setting the result to 0, indicate a static equilibrium. The force balance equation, (6), is obtained by summing these forces together.

$$\int_c^s \mathbf{f}(\xi)\, d\xi \tag{5}$$

$$\mathbf{n}(s) - \mathbf{n}(c) + \int_c^s \mathbf{f}(\xi)\, d\xi = 0 \tag{6}$$

2.5.2 Moment Balance Equation

The moment balance equation is composed of all force applied at a distance and applied torques. Similar to the force balance equation, one moment, (7) results from bending of the rod. There also exists moments created by forces in the rod applied at a distance. They are described in (8) below.

$$\mathbf{m}(s) - \mathbf{m}(c) \tag{7}$$

$$\mathbf{r}(s) \times \mathbf{n}(s) - \mathbf{r}(c) - \mathbf{n}(c) \tag{8}$$

Distributed moments also known as body torques can also be included in the model through the following integral, in (9).

$$\int_c^s \mathbf{l}(\xi)\, d\xi = 0 \tag{9}$$

In the model presented and for the purpose of the verification performed for the model, body torques are not included and are therefore set to zero.

Distributed forces at a distance, such as the torques created by gravity on each individual point of the rod, are also included in the model through the following integral in (10).

$$\int_c^s \mathbf{r}(\xi) \times \mathbf{f}(\xi) d\xi \tag{10}$$

The moment balance equation, (11), is found by summing (7)-(10) and equating the summation to zero:

$$\mathbf{m}(s) - \mathbf{m}(c) + \mathbf{r}(s) \times \mathbf{n}(s) - \mathbf{r}(c) \times \mathbf{n}(c) + \int_c^s \mathbf{r}(\xi) \times \mathbf{f}(\xi) d\xi = 0 \tag{11}$$

2.6 Constitutive Equations

As stated, the constitutive equations combine the kinematics and mechanics by defining the deformation of a specific material resulting from an applied moment or force [21]. The relationship between the deformation and the applied force or moment for some materials obeys a Hookean, linear relationship. One familiar Hookean, linear relationship is $F = kx$, where F is the force applied, k is the spring constant, and k is the displacement of the object of interest. The material used in the verification of this model, Nitinol, obeys a Hookean, linear relationship when at constant temperature and at strains of less than one percent. In order for the model to predict the shape of the rod, constitutive equations along with initial conditions are needed for both forces as well as moments.

The constitutive equation, (13), for the forces consist of the Hookean constant matrix **D** in (12). and the shear displacement matrix in (2). Note that $\mathbf{e}_e$ denotes the axis of rod extension and **D** is a matrix composed of

$$D_1 = D_2 = GA_T, D_3 = EA_T \tag{12}$$

$$\mathbf{n}^l(s) = \mathbf{D}\left(\mathbf{v}^l(s) - \mathbf{e}_e\right) \tag{13}$$

Likewise, the constitutive equation, (15), for the moments consists of the Hookean constant matrix $\mathbf{C}$ in (14). and the bending displacement matrix in (1). Note that $\mathbf{C}$ is a diagonal matrix composed of

$$C_1 = EI_1 \quad C_2 = EI_2 \quad C_3 = GJ \tag{14}$$

$$\mathbf{m}^l(s) = \mathbf{C}\mathbf{u}^l(s) \tag{15}$$

To convert the force and moment constitutive equations to the global reference frame, they are multiplied by **R** and are (16) and (17) respectively.

$$\mathbf{m} = \mathbf{RCu}^l \tag{16}$$

$$\mathbf{n} = \mathbf{RD}\left(\mathbf{v}^l - \mathbf{e}_e\right) \tag{17}$$

2.7 Combining Equations

There are four derivates that must be provided to the ODE in order to solve for the shape of the rod. Two are provided in (3) and (4). The last two are the derivatives of the linear and angular velocities.

The derivative of the linear velocity, $\dot{\mathbf{v}}$, is found by taking the partial derivative with respect to s of (6), substituting the constitutive equation for the forces for $\mathbf{n}$ as well as the result of the body force integral in (18), and solving for $\dot{\mathbf{v}}$, (19).

$$\int_c^s \mathbf{f}\left(\xi\right) d\xi = \rho A g \mathbf{e}_g \tag{18}$$

$$\dot{\mathbf{v}}^l = \mathbf{D}^{-1}\left(\left(-\rho A g \mathbf{R}^T \mathbf{e}_g\right) - \hat{\mathbf{u}}^l \mathbf{D}\left(\mathbf{v}^l - \mathbf{e}_e\right)\right) \tag{19}$$

The derivative of the angular velocity, $\dot{\mathbf{u}}$, is found by taking the partial derivative with respect to s of (11), substituting the constitutive equation for the forces and moments for $\mathbf{n}$ and m as well as $\dot{\mathbf{r}}$ from (3), and solving for $\dot{\mathbf{u}}$, (20).

$$\dot{\mathbf{u}}^l = \mathbf{C}^{-1}\left(-\hat{\mathbf{u}}^l \mathbf{C}\mathbf{u}^l - \hat{\mathbf{v}}^l - \mathbf{D}\left(\mathbf{v}^l - \mathbf{e}_e\right)\right) \tag{20}$$

2.8 Initial conditions

As stated in the above section, initial conditions are needed along with the constitutive equations to solve for the shape of the rod. Initial conditions are the variables that define the initial configuration of the rod. For the model presented, there are four initial conditions. The origin location and initial orientation of the rod must be provided. There is also an initial condition for initial bending which is found iteratively and this process

will be described in the next section. The last initial condition describes the initial shear of the rod and is found analytically using (21). It is derived from the force balance equation by substituting $\mathbf{F}$, the mass applied at the tip, for $\mathbf{n}(s)$, the constitutive equation for **n**, and the body force from (18).

$$\mathbf{v}^{l}(0) = \mathbf{D}^{-1}\mathbf{R}^{T}(0)\left(\mathbf{F} + \rho A g s_{f}\mathbf{e}_{g}\right) + \mathbf{e}_{e} \tag{21}$$

2.9 Matlab Implementation

The model is developed using Matlab, a software package developed for performing calculations using matrixes and vectors. The model presented is developed using an ordinary differential equation solver called ode45 which is available in the Matlab optimization toolbox.

To solve the boundary value problem our model presents, there are several things needed. Initial conditions define the starting conditions for the model and represent, everything about the initial configuration of the system. As previously described, there are four initial conditions. They can be seen in **Error! Reference source not found.**. Initial bending is found iteratively and requires an initial guess. The ODE solver uses the provided initial conditions including this guess and the derivatives to predict a shape for the rod. This bending associated with this shape gives a calculated tip torque, a boundary condition. The torque for the actual system is known based on the mass applied to the tip of the rod and the length of the rod. The two are compared and initial bending is continuously changed until the error between the calculated torque and the actual torque is significantly small. Once the error is small enough, the shape predicted is taken as the correct predicted shape. Verification is then performed on the model by applying multiple

masses to the tip of the actual rod, recording data, and then predicting the shape of the rod with the model by using the same tip masses as detailed in the following chapter.

Table 1

ODE Application

Initial Condition	Meaning	Derivative to Integrate
$\mathbf{r}(0)$	(x, y, z) of rod origin	$\dot{\mathbf{r}}$
$\mathbf{R}(0)$	Initial Orientation	$\dot{\mathbf{R}}$
$\mathbf{u}^l(0)$	Initial bending	$\dot{\mathbf{u}}^l$
$\mathbf{v}^l(0)$	Initial stretch and shear	$\dot{\mathbf{v}}^l$

2.10 Conclusion

Continuum robots are designed to mimic the amazing characteristics of biological structures. There are several models used to control and predict the shape of these robots. One model which uses the constant curvature approximation ignores the significant effects of gravity and thus results for accurate tip control and positioning are very difficult to obtain. Another model based on special Cosserat rods makes few geometrical approximations and no mechanical assumptions. As will be seen in the next Chapter, results

from this approach show that accuracy of the tip position as well as control of the overall continuum robot shape can be obtained using this approach.

A simple free body diagram of the rod provides all information necessary to construct the force and moment balance equations needed for the model presented. Combining the two equations using constitutive equations and along with the initial conditions for the configuration, the initial conditions, and the material parameters, the model can accurately predict the shape of a rod. The model is verified in the Chapter 2.

CHAPTER 3

TWO-DIMENSIONAL MODEL VERIFICATION

3.1 Introduction

As discussed in the previous chapter, special Cosserat rods provide an accurate model which describes the shape of an elastic rod. However, verification of this model must be performed because many applications of a continuum robot, such as minimally invasive surgeries [11], search and rescue operations [5], and colonoscopies [8, 22], require accurate control of the robot tip as well as controlling the physical shape of the robot. Applications of interest to the proposed design include those in which accurate tip position and shape prediction is required. One such design requires the continuum robot to be scaled to a smaller size and used as fingers for a prosthetic hand. Another application for the robot presented in this thesis is a teaching apparatus and a research platform which anyone can construct and use easily in order to teach the fundamentals of continuum robotics. Once verified, the model can be extended to control and verify other continuum robot designs due to its flexibility in parameters.

Verification is the process of using accurate measurements to ensure a designed component works within the specifications given. In this thesis, accurate rod shape and tip coordinates are obtained from a verification setup by attaching a rod to a grid. Tip coordinates are also obtained from the model presented in this work using parameters which match the verification setup, such as material properties, rod orientation, and initial

conditions. Verification of the model is performed by comparing the two data sets. In this chapter, verification of the model proposed in the previous chapter is discussed and results are presented.

3.2 Background

Verification has been performed on the constant curvature models and most results have not been very accurate. In [3], the authors performed verification on the constant curvature model and results show that since the model does not incorporate the significant effects of gravity, poor accuracy is obtained when predicting tip coordinates and rod shape. The model presented in this work incorporates the significant effects of gravity and thus more accurately predicts the shape and tip position of a continuum robot. In [2], the author verifies a model based on special Cosserat rods on OctArm [14]. The results obtained with their model when compared to the constant curvature model were 10 times more accurate [2]. However, Octarm was a mechanically complex continuum robot. It has three pneumatic actuators and has three sections allowing the robot to bend and extend. In contrast, the single section robot to be verified allows bending but not extension. Therefore, Octarm is overly complex compared to what is presented in this work and what is needed for verifying our model.

3.3 2-Dimensional Verification Overview

Verification is the process of using accurate measurements to ensure a designed component works within the specifications given. Tip coordinates are obtained from the proposed model using parameters which match the verification setup, such as material properties, rod orientation, and initial conditions. In this thesis, accurate rod shape and tip

coordinates are obtained from a verification setup by attaching a rod to a grid and lading the tip with a mass. The tip coordinates are recorded and compared to the coordinates from the model. This is comparison is the verification. In this chapter, verification of the model proposed in the previous chapter is discussed and results are presented.

As stated, the model predicts the shape of a robot based on parameters passed to it by the user. The parameters include initial conditions, material properties for the rod, and the mass applied to the rod tip. It is critical that the parameters passed to the model be the same as the physical parameters in order to obtain an accurate prediction of the rod shape; as essential portion of the verification includes determining some of the unknown parameters.

The verification system is as shown in Figure 3, composed of a grid, rod clamps, levels, precision weights, and the rod of interest. The grid is the main component and is what the rod is attached to. The rod is attached using the rod clamps which have different mounting angles etched into them. This allows verification using different initial conditions for orientation. The levels help align the grid to the vertical axis and the precision weights are used to apply the mass to the tip of the rod of interest.

The model is verified using a single rod instead of the actual robot because it simplifies the verification process. This is because if the base model results in erroneous results, it is easier to locate the source of the errors in the model; likewise, there could be errors introduced from the more complex robot (when compared to a single rod), but using a single rod instead drastically minimizes the chances of this because it is the only object that is included in the model whereas with a more complex robot there would be additional complexities that would have to be taken into consideration. In addition, since

the model itself is based on rod theory, instead of complicating the process by changing the base model to incorporate other features of a robot, such as disk guides or cables, first the main component of the robot, a rod, is verified. After verifying the single rod, future work includes extending the model to incorporate a more complex robotic design.

As stated previously, verification of this model must be performed because many applications of a continuum robot require accurate control and precise tip movement. Since the accuracy needed for applications of interest to our research group, the verification is performed using a verification system which has a mm scale grid giving maximum accuracy. This allows the tip position to be read easily and accurately.

As presented in Chapter 4, the material chosen for the backbone of the robot, the rod is a nickel-titanium alloy termed Nitinol (NiTi). NiTi was chosen for its memory shape properties which give it the ability to be very flexible without easily deforming. It is non-deforming as long as strains are less than 1% and the temperature of the rod remains constant. For all verifications, the rod maintained a constant temperature and 1% strains were never reached.

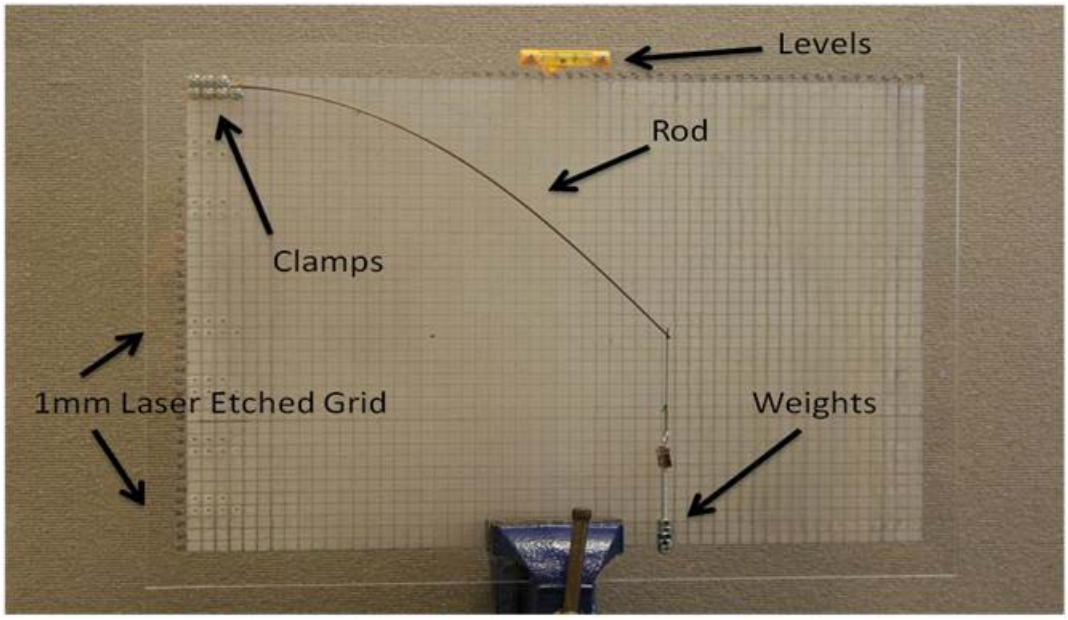

Figure 3 The figure shows the verification system with a mass applied to the tip of a rod. It also shows the components of the verification system which include the grid, levels, clamps, and weights.

3.4 Model Requirements

The model requires parameters associated with the configuration of the robotic system. These parameters include initial conditions and material properties for the rod. Parameters that describe the initial conditions are inputs into the model and as stated in the previous chapter include, location of the origin, robot orientation (axis of extension, which in the verification performed is along the x axis since verification was performed in two dimensions). In all experiments, the rod's base was placed at $(0,0)$m; orientation of 0°, 30°, and 60° from the x axis were also used.

The model requires certain characteristics about the rod material to accurately predict the shape and tip position of a continuum robot. These characteristics include the following: modulus of elasticity, length, diameter and density of the rod material. As stated, the rod chosen for the robot designed and used for verification is NiTi. NiTi was

chosen for its shape memory properties which give it the ability to be very flexible without easily deforming. However, NiTi also has a range for its modulus of elasticity and so the modulus was found by experimentation. The rod length was chosen to be 40 cm and it has a diameter of 1.56 mm. The density was calculated to be 6.80 g/mm^3**.**

The modulus of elasticity for NiTi changes depending on the temperature. To eliminate errors due to guessing, its modulus of elasticity was experimentally found to be 54 GPa. The process used to find the modulus is as follows. First, the rod is attached to the verification system at an initial orientation of 0° and several masses are applied to the tip. The tip coordinates of the deformed rod are recorded. Secondly, the mass used in the setup is entered into the model and $\mathbf{C}_3$ from (14) is modified until the tip coordinate matches the measured tip coordinates. This process is repeated for the other masses. No discrepancies were obtained between any of the masses and the modulus was then calculated using

$$\mathbf{v}^l(0) = \mathbf{D}^{-1}\mathbf{R}^T(0)\left(\mathbf{F} + \rho A g s_f \mathbf{e}_g\right) + \mathbf{e}_e \tag{22}$$

where E is the modulus of elasticity and I is a constant called the second moment of inertia. For all verifications, the rod maintained a constant temperature and 1% strains were never reached.

3.5 Verification Setup Requirements

It is critical to have a very precise verification system to verify the shape and tip predicted by the model. In order to verify the shape and tip positions accurately, one approach is to use a grid, attach the rod or material to it and apply the same parameters to the physical rod as those used in the model, allowing fast, accurate measurement of the

tip position of the rod. Specifically, a 1mm grid was laser-etched on a 80cm x 40cm area, providing ±0.5mm accuracy in measuring tip position. The following sections describe the components of the experimental setup and how they were created to help in obtaining fast and accurate measurements.

The verification system has four main components other than the rod itself. The main component of the system is a laser-etched grid. This grid serves two main purposes. One use is to securely hold the rod during the verification test. The grid was etched with a 1mm grid using a laser cutter. This allows us to easily obtain the tip coordinates of the rod, which is the second purpose of the grid. There are also rod clamps with laser-etched angles. These are used to hold the rod at specified angles which give the rod its orientation. There are two levels mounted at the top of the grid which allow grid alignment with the vertical axis. The last component is the tip mass. The tip mass is a set of precision measured weights which can be applied easily using a small clamp at the tip of the rod.

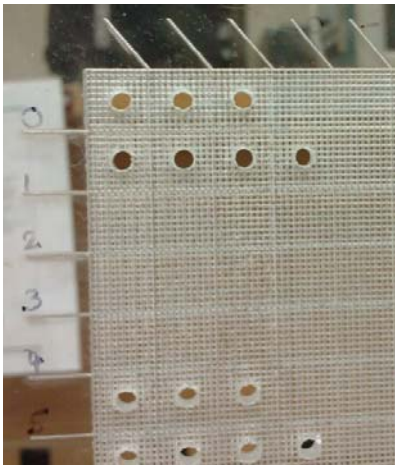

Figure 4 The verification grid is the main component of the verification system. In this figures, a corner is shown with some mounting places for the rod clamps. As you can see, there are etches which create the actual grid. There is 1mm between each and there are a slightly thicker etches every 1cm.

3.5.1 Laser-Etched Grid

The grid is the main component of the verification system. It is used to visually compare the physical rod's deformation to the model's predicted deformation and also to obtain the coordinates for the tip of the rod for comparison with that of the model's. Accurate readings of both are essential in the verification process and are achieved by using a precision cut laser-etched grid. The grid itself is made of acrylic which is a strong, durable, etchable, and easily obtainable material. It is a 45.72 cm x 60.96 cm sheet which is larger than our rod and allows verification of different mounting angles to be performed through the use of rod clamps which are described in the next section. The grid is laser-etched at 1mm increments allowing for maximum resolution when visually obtaining the tip position. There are also seven sets of holes laser-cut to locate them precisely with respect to the grid which are used to attach the rod clamps to the grid. Depending on the orientation of the rod (i.e., mounted at 0 degrees vs. 45 degrees), the rod clamps can be moved accordingly in order to keep the rod tip within the scope of the grid.

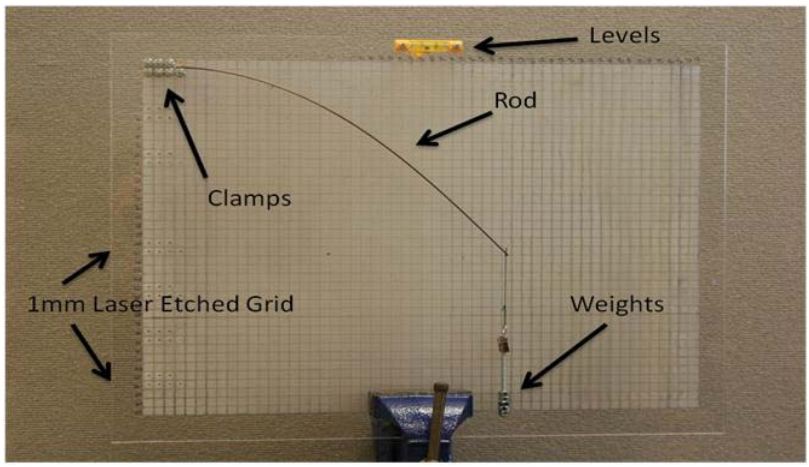

Figure 5 The verification grid can be seen here labeled as 1mm laser etched grid. All components of the verification system are attached to it.

3.5.2 Rod Clamps with Laser-Etched Angles

The rod clamps are used to firmly hold the rod in the chosen orientation during the verification process. This firm hold is essential in obtaining the accurate shape and a tip position reading. A small error in the orientation of the rod amplifies the error between the model and the physical system. Due to the rod orientation being an initial condition for the model, the orientation of the physical system should be exactly, or as close to possible, aligned with the chosen angle. If not the predicted shape from the model cannot account for the discrepancies in orientation and the results will not be accurate. In order to minimize this error, acrylic was chosen and a laser-cutter was used to etch mounting angles into the rod clamps. In addition, the rod is compressed into the chosen mounting angle by placing a non-etched rod clamp on top of the etched rod clamp and then placing screws through threaded holes in the clamps, compressing the rod between the two rod clamps. While it is important to clamp the rod tightly, it is also important that the grid is parallel to the vertical axis to reduce error.

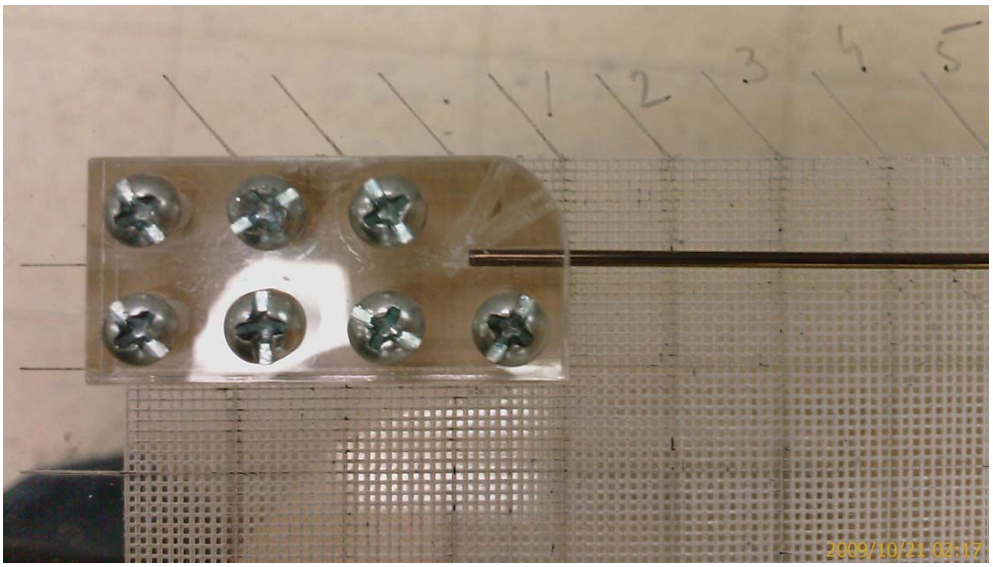

Figure 6 The rod clamping system is shown here. The screws are screwed into tightly tapped holes which compresses the rod into the desired orientation. The clamp shown has 3 orientations etched into it, 0 degrees, 30 degrees, and 60 degrees. Let it be noted that 1cm of the rod length is used for holding the rod in the clamps and this is taken into ac-count in the model.

3.5.3 Levels

It is important that the verification grid is perfectly vertical. Any tilt in the x-y plane or in the y-z plane will introduce directional components which are unaccounted for in the model; therefore, the tip measurements would be inaccurate when compared to the model results. One level is placed parallel to the grid for rotational alignment about the z axis and the other level is placed perpendicular to the grid for rotational alignment about the x axis. Aligning both of these will result in a perfectly vertical, parallel to the y axis, grid which can then be used for accurate verification.

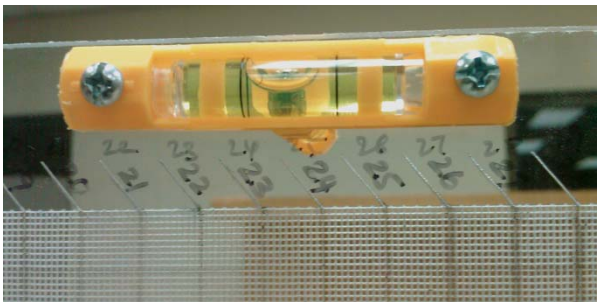

Figure 7 The levels seen here are used to align the verification grid parallel with the ver-tical axis. Two levels are used because the grid can rotate about the x and the z axes; therefore, it must be leveled about two planes.

3.5.4 Precision Measured Weights

During verification of the model, a mass is applied to the model and the resulting coordinates of the predicted shape's tip position is recorded. This is repeated for various weights. These results are then verified by performing the same procedure but with the verification system. One at a time a mass of the same value applied to the model is applied to the physical rod and the result in a tip position for each mass is recorded. If the tip force entered into the model does not correspond to the actual force applied to the physical system then the physical system will not produce results that are comparable to the model. The masses were measured using a pen scale with accuracy of .1 grams and ranged from 13.8 to 41.7 grams.

3.6 Verification Process

In order to verify our model, the following 3-step process was used. The first step in the verification process is to obtain results from the model using various tip masses. Secondly, results from the actual physical system are obtained for the same masses which were used in the model. Lastly, the results from the model and the physical system are compared.

3.6.1 Obtaining Model Results

The objective of this section is to describe the process which was used in obtaining model results. The process begins by entering the necessary parameters into the model. These parameters include initial bending, initial stretch and shear, the axis of extension, the rod mounting angle, the modulus of elasticity (E), the rod length (l), the rod diameter d, and rod density ρ. The values used were $E = 54GPa$, $l = 40cm$, $d = .0445in(1.13mm)$, and $\rho = 6.80\frac{g}{mm^3}$The four of most concern when using the same rod for multiple verifications and setup orientations are rod origin and initial orientation. They can be seen in **Error! Reference source not found.** in Chapter 2.With these parameters the model predicts the corresponding rod shape and output the tip position. The results are shown in **Error! Reference source not found..**

3.6.2 Obtaining Actual Results

The objective of this section is to describe the process which was used in obtaining actual results. The process begins by notching on the tip of the rod in a way that allows a string to be tied. Note that these components were also weighed and added as additional tip force, as shown in Figure 5. This string holds the weights during the verification process. The rod of interest is then clamped at the preferred mounting angle on the verification grid, illustrated in **Error! Reference source not found.**. The grid must be vertically aligned using the levels before any verification can begin; see **Error! Reference source not found.**. One at a time, precision weights are added to the string and the resulting tip positions are recorded.

3.6.3 Comparison of Results

After the results are obtained from both the model and the experimental setup, they are compared. The method used compares the difference in the y offset between the predicted and the observed rod tip coordinates. This value is also represented as a percentage of error compared to the overall length. The results of the predicted model and the actual experimental results are compared and shown in **Error! Reference source not found.**. The average tip error between the predicted rod shape and the actual rod shape is 2.1 mm which equates to 0.61% of the rod's length [21].

Table 2

Results of Model vs Actual

	Predicted		Observed		Error	
Mass (g)	*x* (cm)	*y* (cm)	*x* (cm)	*y* (cm)	In mm	In %
0.00	38.93	-2.16	39.00	-2.30	1.5	0.39
13.80	34.87	-15.94	35.00	-15.90	1.4	0.35
16.90	33.64	-17.98	33.90	-17.80	3.2	0.82
20.00	32.43	-19.71	32.50	-19.50	2.2	0.55
23.10	31.28	-21.16	31.40	-21.20	1.2	0.31
26.20	30.20	-22.40	30.30	-22.40	1.0	0.26
29.30	29.18	-23.47	29.50	-23.30	3.6	0.92
32.40	28.24	-24.38	28.50	-24.40	2.6	0.68
35.50	27.35	-25.17	27.40	-25.40	2.3	0.58
38.60	26.53	-25.86	26.50	-26.20	3.3	0.85
41.70	25.77	-26.48	25.80	-26.90	4.2	1.07
Average					**2.4**	**0.61**

3.6.4 Sources of Error

There are several means by which error can be introduced into the verification system or model. One way that errors can be introduced is from the verification grid not

being perfectly parallel to the y axis. This will induce error because the mass will not apply a tip force completely in the -y direction. Also, if the rod is not held in the exact initial orientation as initialized in the model there will be errors induced. The length of the rod should be carefully measured using a mm scale in order to minimize measurement errors. It is very important that the masses used when applying the tip forces be exactly the same mass that is entered into the model. Any discrepancies between the mass values will induce error into the model. Material property values, such as the modulus of elasticity or density, should be verified to prevent errors also. Lastly, human error can induce inaccuracies into the results of the experimental results by misreading the tip coordinates from the verification grid.

3.7 Conclusion

This chapter shows how important verification is and what approach was taken to verify the model presented in Chapter 2. Given that many of the applications for continuum robots require accurate tip position and control of the entire shape of the body, the model proposed needs to be verified accordingly. Verification was performed on a single rod rather than an entire robot in order to take advantage of the simplest case the model. The model is verified in 2-D and verified by comparing model results to actual experimental results.

The model requires parameters associated with the configuration of the rod including initial conditions which describe the origin location, rod orientation, initial bending, and initial shears. In addition, rod material characteristics are needed for the model accurately predict the physical rod shape.

A verification system was designed in order to obtain the experimental results which were in turn used for verification of the model. The verification system was designed to reduce as many errors as possible and provide consistent experimental result readings with the ease of both in mind. A laser-cutter was utilized in the prototyping of components for precision fabrication and other components (Figure 5), such as precision measured weights and levels, were utilized to reduce errors in the results. The comparisons between predicted and observed results, shown in **Error! Reference source not found.**, show an error of only .61%. Thus, the 3-Dimensional model based on special Cosserat Rods is a viable model for a continuum robot. The following chapter describes the design and construction of a small continuum robot called SCR.

CHAPTER 4

DESIGN AND CONSTRUCTION

4.1 Introduction

This chapter introduces the design for a continuum robot which is used for verifying the model presented in chapter 2. In addition, the model can be used for controlling the robot. As discussed in the previous chapter, the robot design should be simple in order to simplify the verification process. Using a simple rod as the backbone for the robot allows the base model to be verified before it is built upon by adding additional robot components, such as cables and cable guides.

The applications of interest for SCR determined the design in this chapter. First, the application of most importance was to design a continuum robot which could be used as a teaching device. It should be easily assembled and be able to provide a concise understanding, though operation and visualization, of how a continuum robot is different from a rigid link robot. Another application that SCR is designed for is research. This includes verifying a more complex model based on special Cosserat rods derived by extending the current model which was verified in the previous chapter to accurately model the shape of the rod. For example, the model could be extended to 2 or more sections and with this simple design, SCR can also be extended to 2 or more sections. It is a good platform to build upon, which is another consideration that was taken into account when it was designed. Another application includes a scaled-multisection version of SCR used as

fingers for a prosthetic hand. The simple design and the dexterity make the design a viable alternative for prosthetic fingers.

4.2 Background

There are many continuum robot designs that feature excellent control and manipulatibility [2, 10-12, 15]. One design proposed for steerable needles which would be used in minimally invasive surgeries uses curved concentric tubes [10]. By rotating and extending the tubes the shape and length of the continuum robot can be controlled. In addition, by rotating and extending the tubes, the tip position and orientation can be controlled. While highly effective, this design is not feasible for the approaches SCR will is designed for. For instance, SCR is intended to be a platform for research and teaching. It is necessary that the design capture the dexterity of a continuum robot as well as provide a platform for future work and development. The robot is needed to help understand and visualize the basic concepts of a continuum robot for new students, for learning and teaching new concepts, and for continuum robot model verification.

Another continuum robot used for minimally invasive surgery in [11] is designed for laryngeal surgeries. It is a multi-backbone snake like manipulator and has high tip dexterity which enables it to be used for suturing. The design of it uses three snake-like distal dexterity units. This design, while similar to SCR, uses push/pull actuation for manipulating the tip. This introduces complexity into the design that is not wanted because an actuator must be able to push as well as pull. The design of SCR has a single actuator which pulls.

Another design, OctArm V [14, 19] uses pneumatic actuators which require an air source, usually a compressor which is loud and makes the robot bulky. Each section of OctArm is composed of 3 extensible rubber tubes which are actuated by the pneumatic actuators. It would be very difficult to verify our model with OctArm due to its mechanical complexity which would have to be included in the model since the model presented in its simplest form describes a rod.

SCR itself is a modified design of the high-degree of freedom robot (HDOF) continuum trunk proposed and modeled in [23, 24]. The robot in [23, 24], called The Elephant's Trunk, uses a cable servo system similar to the designed proposed in this work; however, one difference is the number of cables and the number and type of actuation mechanisms. While The Elephant Trunk design uses DC motors which need encoders, the robot in this work uses stepper motors for the actuation which provides accurate manipulation without encoders. In addition, manipulation of the robot is performed using 8 cables in addition to springs. While this design is effective, it is also overly complicated and suffers from binding. The chapter introduces a modified design approach to this hyperredundant continuum robot.

The design proposed maintains the overall operation of The Elephant Trunk; however, the complexities are eliminated. By using stepper motors the tip position can be easily and accurately controlled by manipulating the length of the cables and keeping track of the steps. While there can be error introduced to the calculations of cable length it is minimal. Also, the proposed design has only three cables and the springs are eliminated, while full control of the robot of the robot and robot tip was maintained.

4.3 Robot Components

SCR is designed to be used as a research platform for continuum robotics as well as a teaching device for classrooms. In addition, the design is being looked at for prosthetic hand applications. SCR can be easily scaled down, extended to a two section continuum robot, and used as fingers on a prosthetic hand. Given the simplicity of the robot, the model can be easily changed to accommodate another section of SCR.

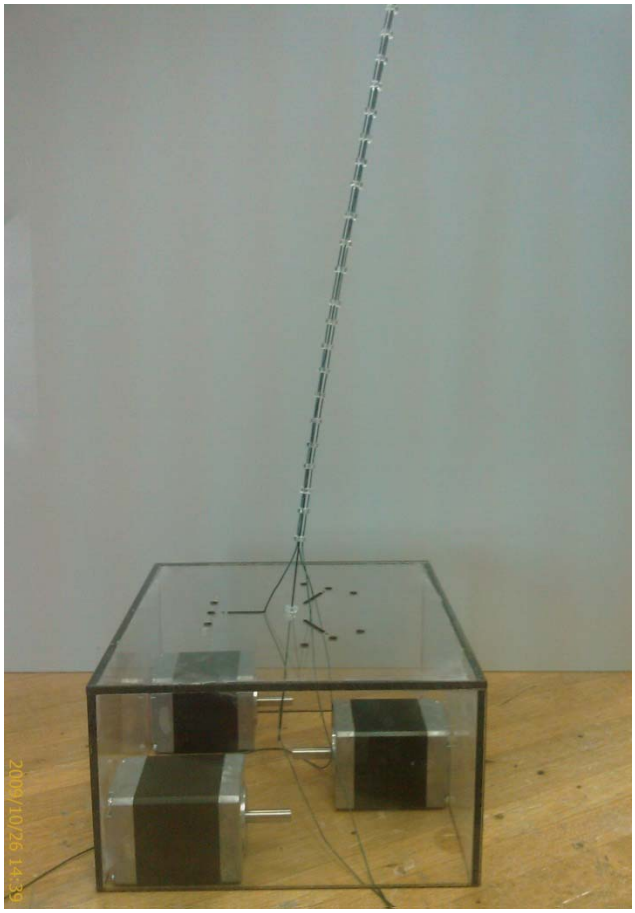

Figure 8 The figure shows the four components of SCR which include a rod, actuation cables, three stepper motors, a base, and cable guides.

The design for SCR is composed of five basic components shown in Figure 8. They include a nickel-titanium (NiTi) rod, actuation cables, three high-torque stepper motors, a base, and acrylic cable guides. Another component of the robot is used in assembly and it's called the assembly device. The main component of SCR is the NiTi rod. It is the backbone of the robot and must be able to support the weight of the cable guides, the control cables, and itself. The cable guides are attached to it at 1cm increments and the cables are passed through the cable guides. The acrylic cables guides are used to ensure that the actuation cables are held parallel to the rod. The actuation cables are used to apply a moment to the tip of the rod for controlling the robot as well as performing tip manipulation. The stepper motors are used to actuate the cables and to help keep track of the length of the cables during operation. A base is used to mount the robot on and house the stepper motors and wiring. Each component is described in more detail in the following sections.

4.3.1 NiTi

As stated, the main component of SCR is the NiTi rod, Figure 9. It is should be able to support itself, the weight of the cable guides, and the actual cables as well as any object that is picked up. Therefore a strong and durable material is needed for the backbone. NiTi is a very strong and flexible metal and is used in many applications such as orthodontics, orthopaedics, medical procedures (i.e., colonoscopies), steerable needles [15], cardiovascular stents, and antennas. NiTi is a shape memory alloy which is excellent for a continuum robot due to its ability to bend without deformation.

Figure 9 The backbone of SCR is a Nickel-Titanium rod (Nitinol) which is a shape memory alloy.

This pseudoelasticity is caused by the modulus of elasticity, diameter to length ratio and NiTi's ability to change crystalline structures. This shape memory effect is possible with NiTi for strains less than 1% at which times plastic deformation will begin to happen. Figure 10 provides additional information.

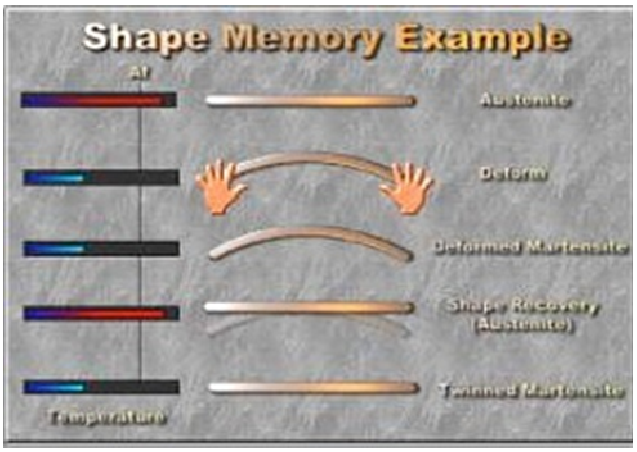

Figure 10 The figure shows how the rod recovers its shape after a deformation occurs. The rod is annealed straight (and at an activation temperature) and this is the austenite phase. At temperatures below the activation temperature the rod is deformable. This is the martensite phase. When the rod is heated to its activation temperature, it returns to austenite phase and becomes straight again.

4.3.2 Actuation Cables

The actuation cables are used to apply a moment to the tip of the rod for controlling the robot as well as for tip manipulation. These cables must be strong enough to not break when the stepper motors are applying large forces on them. They must also be maintained parallel to the rod in order to create a force perpendicular to the rod.

The cables are made of fiber called Dyneema. It is made from polyethylene and is considered to be the world's strongest fiber [25]. It is widely used in fishing, bullet-resistant composites, and medical applications. The fiber is up to 15 times stronger than steel and extremely resistant to abrasion and for these reasons it is used as actuation cables for SCR [25]. The cables are terminated at the tip of SCR on the last cable guide.

The cables are terminated at the tip of SCR on the last cable guide as shown in Figure 11. In order to accurately predict the shape of the rod, the force applied by the cables must be perpendicular to the rod in order to create pure moments.

Figure 11 The figure shows the termination of the cables as well as the cable guides which guide the cables from the motors to the tip in order to apply the tip torque.

4.3.3 Cable Guides

Cable guides are used to ensure the cables are parallel to the rod. They are precision cut by a laser cutter from 1/8 inch acrylic sheets and are designed to press-fit onto the rod. Acrylic was chosen because of its strength. The cable guides are spaced 1cm apart in order to create an overall distribution of the cable guides parallel to the rod. The cables are passed through the holes cut in the cable guides as can be seen in Figure 12.

Initially, the cable guides are approximately placed and then aligned after the cables are passed through all cable guides. There are three actuation cables that are used to manipulate the tip of SCR and likewise, there are three actuation cable holes in each cable guide. The cables are passed through these holes located at 120 degree intervals.

An assembly device is then used to space each disk guide 1 cm apart starting with the tip of the rod.

Figure 12 The figure shows the holes located in the cable guides which the cables pass through from the base to the tip.

4.3.4 Assembly Device

In order to place the cable guides at accurate 1cm spaced increments, an assembly device was designed. Like the cable guides, the assembly device is also precision cut by a laser cutter from 1/8 inch acrylic sheets. At 1cm intervals, the assembly device has rectangular cutouts as seen in Error! Reference source not found. that are used for accurate positioning of the cable guides.

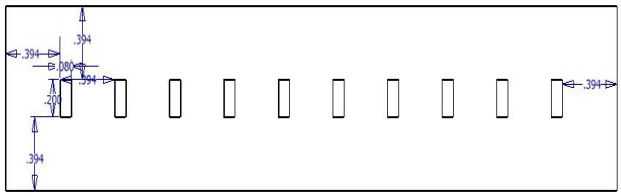

Figure 13 The figure shows a CAD drawing of the assembly device used to space the cable guides at 1 cm increments along the rod.

4.4 Robot Assembly

The assembly of SCR begins with the NiTi rod and the cable guides. The cable guides are press fit into their approximate locations with attention being paid to the alignment of cable holes. After approximate placement of the cable guides, each cable is passed through the appropriate hole in each cable guide from the tip of the robot to the base. When adding the second and third cable, special attention should be given to which hole the cable is being passed through. This is to prevent crossing the actuation cables.

After the cables are in place, the cable guides need to be precisely placed. This means that each disk should be placed 1cm apart and all cable guide holes should be lined up evenly. As stated earlier, this is performed using an assembly device. The assembled rod is placed in the assembly device and each disk is positioned in a corresponding 1 cm spaced rectangular cutout. One cable should be ran across the bottom of the assembly device to help in aligning the cable guide holes.

As stated earlier, the base encases the stepper motors. They are attached to the base using brackets along with screws. The configuration chosen for the stepper motors maximizes the current base size for future development of a two section robot by creating space for additional stepper motors in the same housing, see Error! Reference source not found..

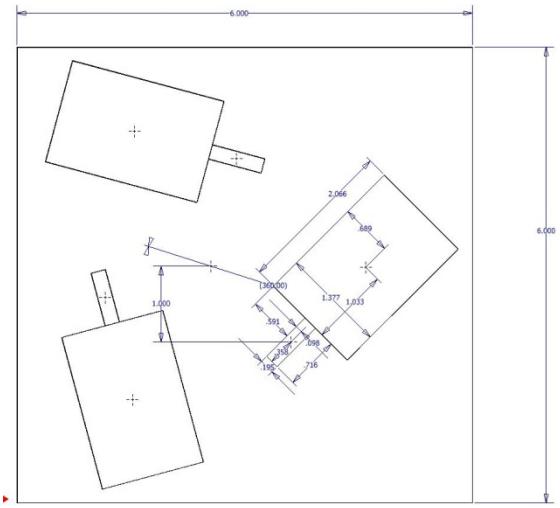

Figure 14 The figure shows the placement of the stepper motors in the base for SCR. The placement is such that pulleys can be used to guide the cables directly from the last cable guide to the stepper motor shafts.

The robot is now ready to be attached to the base. The end of the NiTi rod which does not have the cables terminated is inserted into the center hole on the top of the base, as seen in Error! Reference source not found.**.** The cables are ran through their corresponding holes, placed in the appropriate pulley and terminated at the stepper motor designated for that cable.

The NiTi rod must also be rigidly attached to the base. This is achieved by using epoxy glue to attach extra disk guides to the end of the rod above the base and repeating this procedure on the underside of the base.

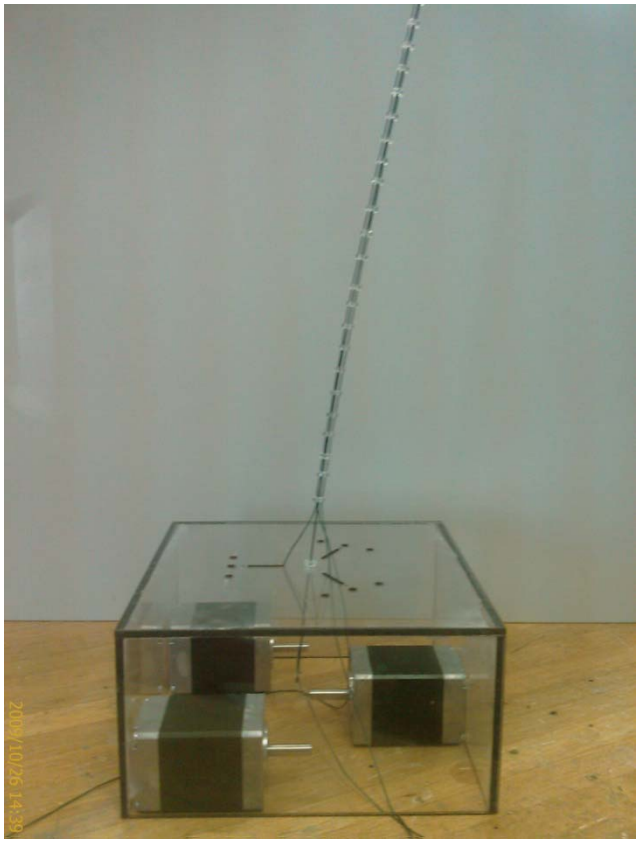

Figure 15 The figure shows the base which SCR is attached to. The stepper motors are also housed in this and can be seen.

4.5 Conclusion

This chapter discussed the design for a continuum robot which is used for verifying the model presented in chapter 2. The robot design is simple in order to simplify the verification process. A single NiTi rod is used for the backbone of the robot because of its memory shape ability. Cable guides are press-fit onto the rod and are used to run the actuation cables through. The actuation cables are used to apply a force on the tip which creates a moment for tip manipulation. The cable guides are placed 1cm apart and are done so using an assembly device. The assembled robot is attached to the base which houses three stepper motors used for actuation.

The design of SCR is a viable solution for the applications presented in the work. This design would make an excellent teaching utensil in the area of continuum robotics. It is simple to build and it would be feasible for the entire robot to be built by each student in a class. The design can also be implemented by research groups who have little to no understanding of continuum robots, but who are interested in starting in the area; in contrast, a research group who has worked with continuum robotics for some time, can easily use the robot for new and perhaps more complex model verifications, continuum robot applications, and proof of concept research. In conclusion, the robot designed and proposed in this chapter is a viable design which can be used in many applications in the continuum robot community, especially those of interest to the MSU Robotics Research group.

CHAPTER 5

CONCLUSION AND FUTURE WORK

5.1 Conclusion

Continuum robots are remarkable creations with inspirations coming from many biological structures. This thesis presents a contribution to the modeling of continuum robots, the verification of this model, and discusses a verification platform for verifying continuum robots, in addition to presenting a simple and controllable continuum robot which demonstrates dexterity and compliancy. The disadvantage of existing models is analyzed and the proposed model was presented. The model presented makes few geometrical approximations or mechanical assumptions and therefore includes the significant effect of gravity on a robotic system.

A verification system was presented and verification of the model was performed. The system was designed for quick, easy, and most importantly accurate tip position coordinate readings. Accuracy was achieved by using a laser-cutter to etch a 1mm grid onto a sheet of acrylic and to create mounting angles in the rod clamps. These rod clamps allows accurate rod mounting at desired angles. These accurate tools used to create the system solved many issues which were present in previous versions of the verification system. The process provides for the experimental determination of the modulus of elasticity of the rod of 54GPa. Using this result, low model errors of 0.61% demonstrate the validity of the model.

Finally, the robot presented in the final chapter is a modification of an existing design. The design was simplified without sacrificing the most important aspects of the robot which include accuracy and controllability. For example, one design was overly complex with pneumatic actuators and remote compressors used for actuating the robot trunk. Another design, the one which was modified, reduces the complexity by removing DOF achieved by additional cables and springs. While reducing the number of cables and springs, controllability was maintained and the robot was simplified. This robot is an excellent design which can be used for a research group interested in working with continuum robotics, professors interested in teaching robotics, and design engineers looking to add dexterity to an existing design, such as a prosthetic hand.

5.2 Future Work

The work presented is the foundation for much more work that needs to be performed. Future work includes a control system for the single-section continuum robot designed and expanding the robot design to a multisection robot. There will also be a need for a control system for a multisection robot once the single section robot is finished and controllable.

The model is in the process of being expanded to incorporate all components of the robot, including disk guide and cable weights. Predicting dynamics of a continuum robot is the next important step for the model and once completed, the model should be extended to a multisection static and then multisection dynamic model.

Finally extension of the verification procedure to provide verification in three-dimensions will be performed. A setup called visual servoing uses a pair of cameras to

determine the robot shape or robot tip position based on geometry. The system can also be used for controlling the robot.

REFERENCES

[1] M. W. Hannan and I. D. Walker, "Kinematics and the Implementation of an elephant's trunk manipulator and other continuum style robots," *Journal of Robotic Systems,* vol. 20, pp. 45-63, Feb. 2003.

[2] D. Trivedi, A. Lotfi, and C. D. Rahn, "Geometrically exact dynamic models for soft robotic manipulators," in *IEEE/RSJ International Conference on Intelligent Robots and Systems*, San Diego, CA, 2007, pp. 1497-1502.

[3] S. Neppalli and B. A. Jones, "Design, Construction, and Analysis of a Continuum Robot," in *Proceedings of the International Conference on Intelligent Robots and Systems*, San Diego, CA, USA, 2007, pp. 1503-1507.

[4] R. Cieslak and A. Morecki, "Elephant trunk type elastic manipulator – a tool for bulk and liquid type materials transportation," *Robotica,* vol. 17, pp. 11-16, 1999.

[5] H. Tsukagoshi, A. Kitagawa, and M. Segawa, "Active Hose: an artificial elephant's nose with maneuverability for rescue operation," in *Proceedings of the IEEE International Conference on Robotics and Automation*, Seoul, Korea, 2001, pp. 2454-2459.

[6] S. Ma, S. Hirose, and H. Yoshinada, "Development of a Hyper-redundant Multi-joint Manipulator for Maintenance of Nuclear Reactors," *International Journal of Advanced Robotics,* vol. 9, pp. 281-300, June 1995.

[7] R. J. Webster, III, J. S. Kim, N. J. Cowan, G. S. Chirikjian, and A. M. Okamura, "Nonholonomic Modeling of Needle Steering," *The International Journal of Robotics Research,* vol. 25, pp. 509-525, May 1 2006.

[8] G. Chen, M. T. Pham, and T. Redarce, "Development and kinematic analysis of a silicone-rubber bending tip for colonoscopy," in *Proceedings of the IEEE/RSJ International Conference on Intelligent Robots and Systems*, Beijing, China, 2006, pp. 168-173.

[9] S. J. Phee, W. S. Ng, I. M. Chen, F. Seow-Choen, and B. L. Davies, "Locomotion and steering aspects in automation of colonoscopy. I. A literature review," *Engineering in Medicine and Biology Magazine, IEEE,* vol. 16, pp. 85-96, 1997.

[10] P. Sears and P. Dupont, "A Steerable Needle Technology Using Curved Concentric Tubes," in *Proceedings of the IEEE/RSJ International Conference on Intelligent Robots and Systems*, Beijing, China, 2006, pp. 2850-2856.

[11] N. Simaan, R. Taylor, and P. Flint, "A dexterous system for laryngeal surgery," in *Proceedings of the IEEE International Conference on Robotics and Automation*, 2004, pp. 351-357 Vol.1.

[12] N. Simaan, "Snake-Like Units Using Flexible Backbones and Actuation Redundancy for Enhanced Miniaturization," in *Proceedings of the IEEE International Conference on Robotics and Automation*, Barcelona, Spain, 2005, pp. 3023-3028.

[13] W. M. Kier and K. K. Smith, "Tongues, tentacles and trunks: the biomechanics of movement in muscular-hydrostats," *Zoological Journal of the Linnean Society,* vol. 83, pp. 307-324, 1985.

[14] S. Neppalli, B. A. Jones, M. Csencsits, W. McMahan, V. Chitrakaran, M. Grissom, M. Pritts, C. D. Rahn, and I. D. Walker, "OctArm - Soft Robotic Manipulator," in *video in Proceedings of the International Conference on Intelligent Robots and Systems* San Diego, CA, USA, 2007.

[15] R. J. Webster, A. M. Okamura, and N. J. Cowan, "Toward Active Cannulas: Miniature Snake-Like Surgical Robots," in *IEEE/RSJ International Conference on Intelligent Robots and Systems*, Beijing, China, 2006, pp. 2857-2863.

[16] Y. Bailly and Y. Amirat, "Modeling and Control of a Hybrid Continuum Active Catheter for Aortic Aneurysm Treatment," in *Proceedings of the IEEE International Conference on Robotics and Automation*, Barcelona, Spain, 2005, pp. 936-941.

[17] B. A. Jones and I. D. Walker, "Kinematics for Multisection Continuum Robots," *IEEE Transactions on Robotics,* vol. 22, pp. 43-55, Feb. 2006.

[18] B. A. Jones and I. D. Walker, "Practical Kinematics for Real-Time Implementation of Continuum Robots," *IEEE Transactions on Robotics,* vol. 22, pp. 1087-1099, Dec. 2006.

[19] B. A. Jones, M. Csencsits, W. McMahan, V. Chitrakaran, M. Grissom, M. Pritts, C. D. Rahn, and I. D. Walker, "Grasping, manipulation, and exploration tasks with the OctArm continuum manipulator," in *video in Proceedings of the International Conference on Robotics and Automation*, Orlando, FL, USA, 2006.

[20] S. S. Antman, *Nonlinear problems of elasticity*, 2nd ed. New York: Springer, 2005.

[21] B. A. Jones, R. L. Gray, and K. Turlapati, "Three Dimensional Statics for Continuum Robotics," in *IEEE/RSJ International Conference on Robots and Intelligent Systems*, St. Louis, Missouri, USA, 2009, pp. 2659-2664.

[22] F. Thomann, M. Betemps, and T. Redarce, "The development of a bendable colonoscopic tip," in *International Conference on Robotics and Automation*, Taipei, Taiwan, 2003, pp. 658-663.

[23] I. D. Walker and M. W. Hannan, "A novel `elephant's trunk' robot," in *Advanced Intelligent Mechatronics, 1999. Proceedings. 1999 IEEE/ASME International Conference on*, 1999, pp. 410-415.

[24] I. A. Gravagne and I. D. Walker, "Kinematic transformations for remotely-actuated planar continuum robots," in *Robotics and Automation, 2000. Proceedings. ICRA '00. IEEE International Conference on*, 2000, pp. 19-26 vol.1.

[25] D. C. Dyneema, "Dyneem, The World's Strongest Fiber," 2009.